Recent developments in cryo-electron microscopy reconstruction of single particles

Yizhi Tao* and Wei Zhang†

Cryo-electron microscopy and single-particle 3D image reconstruction techniques have been used to examine a broad spectrum of samples ranging from 500 kDa protein complexes to large subcellular organelles. The attainable resolution has improved rapidly over the past few years. Structures of both symmetric and asymmetric assemblies at approximately 7.5 Å have been reported. Together with X-ray crystallography, three-dimensional cryo-electron microscopy reconstruction has provided important insights into the function of many biological systems in their native biochemical contexts.

Addresses
*Department of Molecular and Cellular Biology, 7 Divinity Avenue, Harvard University, Cambridge, MA 02138, USA; e-mail: tao@crystal.harvard.edu
†Department of Biological Sciences, Purdue University, West Lafayette, IN 47907, USA; e-mail: leila@bragg.bio.purdue.edu

Current Opinion in Structural Biology 2000, **10**:616–622

0959-440X/00/$ – see front matter

Abbreviations

2D	two-dimensional
3D	three-dimensional
CCD	charge-coupled device
CTF	contrast transfer function
ds	double-stranded
EM	electron microscopy/microscope
NCS	noncrystallographic symmetry
TEM	transmission EM

Introduction

Using better sample preparation, more advanced instrumentation, better imaging techniques and more robust algorithms, the resolution of 3D cryo-electron microscopy (cryo-EM) reconstruction has been constantly improved over the years. Today, cryo-EM reconstruction has become a powerful tool in determining the 3D structure of macromolecules at nanometer or even subnanometer resolution [1••,2••]. If well-ordered, helical or 2D crystalline specimens are available, near-atomic resolution can be achieved and the biological function of the studied molecule can be understood in atomic detail [3•,4••,5,6•,7•,8]. In the more general case of single-particle reconstruction, structures at resolutions higher than 10 Å have been reported [9]. Although it is difficult to recognize individual amino acid residues at this resolution, researchers can derive important information regarding protein domain arrangements or can even be able to trace the polypeptide chain [9].

Compared with X-ray crystallography and NMR methods, cryo-EM, combined with 3D image reconstruction techniques, offers some distinct advantages:

1. Many forms of specimen (e.g. helical, 2D crystalline or even single particles) can be examined. Large assemblies and complexes, with dimensions of 30–200 nm, are especially suitable for structural study by cryo-EM reconstruction.

2. In many cases, nonhomogeneous samples can be studied as a homologous group can be manually selected from cryo-EM micrographs.

3. Time-resolved studies can be carried out more easily because biochemical reactions can be terminated at a preferred time point by flash freezing.

4. Phase information for the structure is retained as the diffracted electron beam is refocused to form a real-space image on an image plane.

5. It is more efficient; in optimal cases, reconstruction at medium resolution (~20 Å) can be obtained in one week.

With the above advantages, the combination of EM reconstruction with X-ray crystallography and NMR spectroscopy enables structural biologists to gain a much more comprehensive understanding of the studied molecule than could possibly be achieved with any single technique [10•]. EM reconstruction can be interpreted in greater precision by fitting an X-ray model into an EM density map [11,12,13•]. On the other hand, an EM reconstruction at low resolution (~20 Å) can be used as a phasing model in solving crystallographic structures of viruses or macromolecules [14,15,16•,17,18].

For different forms of specimen (e.g. helical, 2D crystalline or single particles, and symmetric or asymmetric objects), practical strategies for sample preparation, data collection and data merging are vastly different. The following sections discuss recent progress made in the field of single-particle reconstruction. The review by Yeager *et al.* [3•] should be consulted for a discussion of electron crystallography of 2D crystals. The article by DeRosier *et al.* [19] provides an update on the reconstruction of helical specimens.

General procedures for single-particle 3D cryo-electron microscopy reconstruction

Single-particle cryo-EM reconstruction generally involves the following steps [20••]. First, the preparation of the vitrified samples. Biological specimens suitable for cryo-EM are flash-frozen on holey carbon-coated grids in liquid ethane and are subsequently maintained at liquid nitrogen or helium temperature after being transferred to a cryo-sample holder in the EM. Second, the collection of EM images. Specimen areas that have thin vitreous ice

and evenly distributed particles are located and photographed on an emulsion film or recorded by a charge-coupled device (CCD) detector [21•]. Third, the determination of particle parameters. Single-particle images are collected from digitized micrographs. The spatial relationship between different particles can be defined by three Eulerian angles that define the orientation and two translational elements that define the position of the particle. Four, 3D reconstruction. As a result of the large depth of field, a transmission EM (TEM) image of a thin specimen is a projected view of the object along the optical axis. Either the reverse Fourier transform method or the back-projection method [22] can be used to reconstruct a 3D structure from images of particles that are variously oriented. Five, the refinement of particle parameters. In model-based refinement approaches, projections of the initial reconstruction are used to refine particle parameters and the newly calculated reconstruction is then used for the next round of refinement. The cycle continues until the correlation between model projections and raw images converges. Six, resolution improvement. In cryo-EM, a slight underfocus is usually used to generate phase contrast for biological specimens, which inherently have a low scattering power [20••]. Although the object is more readily visible, the Fourier transform of the resulting image is modulated by the 'contrast transfer function' (CTF) (see Figure 1). To calculate a reconstruction at high resolution, not only must phases be reversed in alternate resolution regions, but amplitudes also need to be rescaled to compensate for the diminishing effect whenever the CTF function passes zero. Seven, resolution assessment and structure interpretation. The effective resolution of the reconstruction is assessed by determining the consistency of two independent reconstruction maps in reciprocal space as a function of resolution.

Figure 1

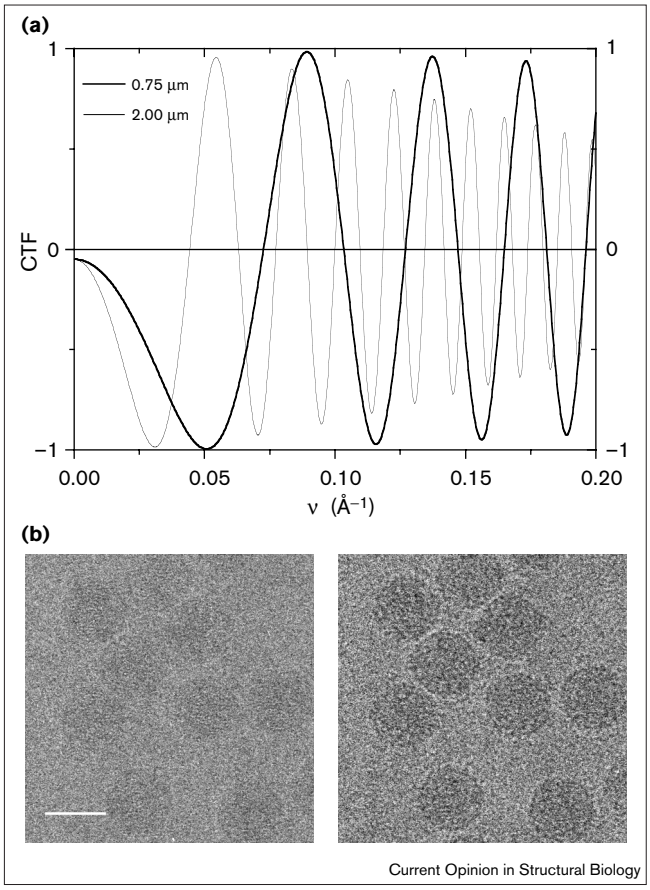

Contrast transfer function (CTF). **(a)** CTF plotted against spatial frequency (ν). The microscope is operated at 200 kV, with a source size of 0.005 Å^{-1} and an energy spread of 0.5 eV [1••]. The spherical aberration is 2.0 mm. The amplitude contrast is assumed to be 0.05. The thick line and the thin line correspond to an underfocus level of 0.75 μm and 2.00 μm, respectively. The finite source size and nonmonochromatic electron beam both cause Gaussian decay of the CTF [82]. In practice, contrast is much weaker at high spatial frequencies as a result of further decay caused by other factors, like inelastic scattering, specimen drift and beam-induced charging [60•]. Magnetic lens astigmatism produces an anisotropic CTF that varies with direction in 2D Fourier transform. The position where the CTF traverses the zero point is called a node. **(b)** Cryo-EM micrographs of the same field of reovirus cores taken at different underfocus levels: left, 1.52 μm; right, 3.49 μm. Scale bar represents 50 nm. (Micrographs courtesy of NH Olson and TS Baker, Purdue University.)

Recent developments

Sample diversity

Viruses

For viruses with icosahedral symmetry, studies on structure and assembly, neutralization, receptor recognition and cell entry have been carried out [9,11,12,20••,23,24,25•,26,27]. Nonicosahedral viruses are now also being studied. Bacteriophage ϕ29, which consists of a prolate, fivefold head and a tail assembly attached to a fivefold vertex of the head, was reconstructed to 27 Å resolution [28,29]. The DNA packaging portal, which is situated at a fivefold axis in dsDNA phages and had been unresolved in previous reconstructions using icosahedral averaging, was visualized *in situ*. The structure of maize streak virus, a type of Geminivirus, has also been established to 25 Å resolution [30•]. This model demonstrated that a Geminivirus consists of two incomplete T = 1 icosahedra with 52 point group symmetry. The handedness of a Geminivirus particle was also determined (W Zhang, TS Baker, unpublished data). In a situation in which the symmetry of the object is low, yet no structural information is available, a new procedure suggested by Rossmann and Tao [31•] could help to determine the best orientation on the basis of the self-rotation function of the object. In contrast to the common-lines method [32], which uses only Fourier coefficients along symmetry-related lines, this procedure utilizes the complete 2D projection data. Experiments on noise-free data showed that the orientation could be accurately determined using information presented by just fivefold symmetry in the structure.

Particles with no symmetry or low symmetry

3D EM reconstruction has been applied to many molecules other than viruses, some with various kinds of

symmetry and some with no symmetry at all. Examples include the eukaryotic ribosome–EF2 complex (onefold) [33], the ATP-dependent protease ClpAP (six and sevenfold) [34], chaperonin CCT (eightfold) [35•], human transcription factor IID complexed with TFIIA(IIA) and TFIIB(IIB) (TFIID–IIA–IIB) (onefold) [36], the plant photosystem II supercomplex (twofold) [37], ryanodine receptor/calcium release channel (RyR3) (fourfold) [38], the portal complex of bacteriophage SPP1 (13-fold) [39], the membrane pore formed by α-latrotoxin (fourfold) [40] and a cellular vault (eightfold) [41]. For a detailed discussion on the ribosome, interested readers should go to a recent review by van Heel [42]. Currently, the only limitation of single-particle reconstruction seems to be a minimum particle size of approximately 500 kDa. Reconstruction of smaller objects is usually problematic, although, in principle, reconstruction of smaller macromolecules is possible [43].

Objects with symmetry mismatches

Cryo-EM reconstruction is also a powerful tool in studying objects with some asymmetric features [31•]. Frequently, the distribution of some structural elements in a complex assembly deviates from the overall symmetry of the object. For example, both the binding of an unfolded polypeptide to a chaperonin molecule and the attachment of a 12- or 13-fold symmetric connector to a fivefold axis of dsDNA phage involve some kind of symmetry mismatch. As the unique binding sites involved are usually related to important biological functions, it is of interest to study their detailed structure. In crystals, these asymmetric portions may not be involved in crystal contacts and may be disordered with respect to the crystal lattice, so they will not be visible in electron density maps. EM reconstruction of single particles, however, does not perform translational averaging, which is inherent in X-ray crystallography. Reconstruction of objects with small symmetry-mismatched features can be obtained by pre-aligning particles through the symmetric part of the structure before accurately aligning them on the basis of small asymmetric features (Y Tao, TS Baker, MG Rossmann, unpublished data). A recent example of an object with symmetry-mismatched features that has been studied by cryo-EM is bacteriophage ϕ6. It was shown that, in phage ϕ6, a sixfold symmetric polymerase complex attaches to each fivefold vertex of the virus [44•]. The interaction between the eukaryotic type II chaperonin CCT and its actin substrate was also visualized by studying their complex structure [35•].

Samples demonstrating dynamic behavior

Another advantage of EM reconstruction is that it is convenient in studying dynamic biological problems. In crystallography, time-resolved studies using Laue diffraction are difficult and only rarely possible [45]. The key problem is the necessity that all molecules in a crystal change synchronously and that the conformational changes do not disturb the regular crystal lattice. In cryo-EM, structural changes do not have to be precisely synchronized. Biochemical reactions can be terminated by cryo-freezing and particles that appear to have distinct conformations can be manually grouped to avoid interference from each other. Therefore, snapshots of intermediates along the reaction pathway can be obtained by 3D reconstruction [46]. Several perturbation devices facilitate kinetic cryo-EM studies [1••]. The recent invention of a spray-freezing apparatus provides a timing control that can be as accurate as several milliseconds [47]. A fast-freezing device with a retractable chamber is useful when it is important to control environmental variables such as humidity and temperature [48].

Studies of dynamic behavior are best illustrated by the recent work on bacteriophage HK97 [49•]. The maturation of phage HK97 from the prohead can be simulated *in vitro* by lowering the pH. A total of five reconstructions corresponding to different intermediate stages showed how the prohead rearranges its capsid protein and eventually matures into a virion. The extensive conformational change of the ribosome during tRNA translocation was also studied by EM reconstruction [50•]. The reaction mixture was allowed to proceed to different extents in the formation of pre-translocational and post-translocational complexes. A comparison of reconstructions of these two states suggested possible translocation mechanisms.

Subcellular organelles

There have been exciting developments recently in electron tomography [51], especially as applied to problems in the field of cell biology. In tomography, a reconstruction is obtained from a tilt series of a single particle. Therefore, tomography is usually the method of choice when there are so many structural variations that averaging among particles is not possible. Subcellular organelles, well preserved in their native form and native environment by flash freezing, are especially suitable for this kind of study because of interparticle variations. Recent 3D reconstructions of mitochondria [52•] and the Golgi complex [53] revealed a lot of structural details that cannot be observed by traditional TEM. However, the resolution of tomography currently seems limited to approximately 2.8 nm as a result of radiation damage [4••].

Pushing the resolution limit

Recently, several structures have been established to beyond 10 Å resolution using single-particle cryo-EM reconstruction. These include the hepatitis B viral capsid (~32 nm in diameter) [9,54], the bovine papillomavirus (~60 nm in diameter) [55], the Semliki Forest virus (~70 nm in diameter) [56], the *E. coli* ribosome large subunit (~15 nm in size) [57•] and the herpesvirus capsid (~125 nm in diameter) [58•]. Also, the structure of the 70S ribosome was solved to 11.5 Å resolution [59]. Whereas the hepatitis B viral capsid, the papillomavirus, the Semliki Forest virus and the herpesvirus capsid have icosahedral symmetry, ribosome molecules are completely asymmetric. These structures demonstrate the potential of EM reconstruction in providing high-resolution structural

information. The impressive improvement in resolution arises from the following technical advances. First, field emission gun illumination sources improve both the spatial and temporal coherence of the electron beam, thus significantly increasing the resolution of the information contained in TEM images. Second, more accurate CTF correction techniques have been developed [9,60•]. Third, significantly more images recorded at different defocus levels are included to fill in the missing data at CTF nodes, to boost the signal-to-noise ratio at all resolutions and to compensate for possible radiation damage in some particles [59]. Viruses are good objects for high-resolution studies because of their high internal symmetry. For objects with lower symmetry or no symmetry at all, more images are required to obtain reconstructions of similar quality. For instance, approximately 16,000 particles were used for the 7.5 Å resolution reconstruction of the 50S ribosomal subunit [57•], compared with the approximately 600 images used for the hepatitis B viral capsid [9].

To further improve the current resolution limit, several factors, for example, the CTF correction, the electron beam accelerating voltage and the beam-induced charging effect, have been addressed recently. Given the most optimal microscope conditions, more precise CTF correction is one of the most important considerations. Structure factor comparison between an EM reconstruction and a crystallographic structure of the ribosome at the same resolution shows that the Fourier amplitudes were progressively underestimated at higher resolution [61•]. It was shown that using the solution X-ray scattering intensity for amplitude scaling yielded a reconstruction with better high-resolution structural details [62•]. In addition, it was noticed that the underfocus level changes with the height of the specimen and results in nonuniform CTFs for different parts of the structure. The nonuniform CTF causes a loss of contrast for high-resolution data that is especially severe when the studied object has a large dimension. To alleviate this problem, a 400 kV accelerating voltage was used in studying the rather large capsid of herpesvirus [58•]. Another problem is sample heterogeneity, as an isolated particle is likely to have more structural flexibility than a crystalline sample constrained by lattice contacts. Thus, stricter particle selection criteria might be helpful [54]. Moreover, beam-induced specimen charging causes a loss of high-resolution data. It was found that conductive surface coating effectively reduces charging on unsupported specimens [63].

Complementing crystallography

In many cases, the power of cryo-EM reconstruction lies in the possibility that it can be used to study structures of large complex assemblies or to visualize interactions of macromolecules in action. Although the relatively low resolution of a reconstruction may not allow the direct recognition of amino acid residues or nucleotides, the structure can be interpreted beyond the resolution limit of the electron density map if the atomic structures of smaller components are available. In the past, many pseudo-atomic structures were obtained by fitting the coordinates of their components into the 3D maps of the complexes (for recent examples, see [11,12,13•,26]). The fitting of an atomic model can be facilitated or confirmed in a variety of ways:

1. Heavy-atom labeling (see issue 127 of the *Journal of Structural Biology* for complete coverage). For example, undecagold can be used to locate cysteine [64] and Ni–NTA–gold clusters selectively target histidine-tagged proteins [65].

2. Site-directed mutagenesis. With proper manipulation, the insertion or deletion of a small piece of peptide, DNA or RNA can be used to identify termini or specific sites in surface loop regions of macromolecules [66,67].

3. Antibody labeling. Monoclonal antibodies can be used to locate peptide motifs on the protein surface [68].

4. For nucleic acids, cross-linking and footprinting data are useful [13•].

5. For glycoproteins, the location of the sugar moiety is informative [69].

On the other hand, 3D EM reconstruction continues to complement crystallography as an aid to structure determination. Using phases from EM reconstruction at relatively low resolution, a high-resolution X-ray structure can be determined through various means of density modification (e.g. solvent flattening and noncrystallographic symmetry [NCS] averaging [70]). Recent examples include the blue tongue virus core, with 30-fold NCS [14], the reovirus core, with fivefold averaging [16•], the Norwalk virus capsid, with 30-fold averaging [15], and ClpP, with sevenfold rotational symmetry [17]. Even with no NCS present, the 3D reconstruction of the ribosome at 20 Å resolution was used successfully to locate particles in unit cells and subsequently to help in phasing difference Fourier maps of heavy-atom derivatives [18].

Automation and software development

Automation of the reconstruction procedure has been undergoing development recently. Reconstruction at high resolution generally requires 10^4 or even 10^5 particle images; therefore, it is important to develop automated procedures for labor-intensive work. A web-based TEM control interface for automated data acquisition was recently developed [71,72]. Carbon grids with precisely positioned holes [73] and a goniometer with better relocation precision [74] both facilitate computer-controlled image recording. Particle selection, which can be tedious, has also been automated in a number of cases [72,75,76]. For refinement, parallel processes speed up calculations [77]. Automated algorithms for fitting atomic models into EM maps are also available [78,79], although some manual intervention is necessary.

Over the years, many laboratories have developed their own reconstruction software for tackling their special biological problems, such as highly symmetric or asymmetric objects, and model-based or random conical tilt methods. To facilitate software sharing and development, there is an outreach program with a web site at http://emoutreach.sdsc.edu [80]. In addition, a universal conversion tool (EM2EM: http://www.imagescience.de/em2em/) is available to handle different map formats, so that structures solved in different laboratories can be compared. Meanwhile, more attention has been drawn to the issue of establishing a database with all available 3D images to allow more convenient access. The BioImage database project has a web site at http://www.bioimage.org [81•].

Conclusions

Cryo-TEM 3D reconstruction is a powerful tool in studying the native structure of protein complexes and subcellular organelles. At the moment, many macromolecules from 10 nm to 200 nm have been studied successfully to resolutions at nanometer or even subnanometer level. The recent reconstruction of the *E. coli* ribosome large subunit at 7.5 Å resolution shows that asymmetric macromolecules with important biological functions can be routinely studied at 10–30 Å resolution. Theoretical estimates indicate that particles as small as 100 kDa should provide enough contrast for alignment if imaging techniques can be improved [43].

Pushing the resolution of a reconstruction beyond 5 Å remains a challenge in the field of cryo-TEM single-particle reconstruction. Many factors are worthy of consideration. Improvements in instrumentation, like higher voltage (400 kV), helium-cooled cryo-stages, energy filters and field emission guns, help to preserve biological specimens and to record images with stronger phase contrast. Meanwhile, algorithms are needed for more accurate particle alignment (orientation parameters and translational elements). CTF parameters need to be determined for individual images as the defocus level may vary across the whole EM film. A careful CTF correction algorithm is especially important for data around CTF nodes, where the signal is very weak. Furthermore, microscope astigmatism and specimen drift need to be assessed and computationally corrected (TS Baker, personal communication). Given the fast pace of the recent developments, the first atomic structure of a single particle by 3D cryo-EM reconstruction is probably only just around the corner.

Update

A review on icosahedral virus structure determination was published recently [83•].

Acknowledgements

We sincerely thank Karin M Reinisch, Timothy S Baker, Michael G Rossmann, Stephen C Harrison and Qing R Fan for their helpful comments on the manuscript. We thank Yu Chen for his help with Figure 1. This manuscript is supported by National Institutes of Health grant number GM33050 to Timothy S Baker. W Zhang is a recipient of the Purdue Research Foundation fellowship.

References and recommended reading

Papers of particular interest, published within the annual period of review, have been highlighted as:

- • of special interest
- •• of outstanding interest

1. Baker T, Henderson R: **Electron cryomicroscopy.** In *International Tables for Crystallography*, vol F. Edited by Rossmann M, Arnold E. Dordrecht: Kluwer Academic Publishers; 2000:in press.
•• This review describes 3D electron microscopy procedures for studying helical particles, 2D crystals and single particles.

2. Chiu W, McGough A, Sherman M, Schmid MF: **High-resolution electron cryomicroscopy of macromolecular assemblies.** *Trends Cell Biol* 1999, **9**:154-159.
•• This review evaluates the potential of electron cryomicroscopy in obtaining high-resolution structures. Examples are given to demonstrate the versatility of this technique in studying complex biomacromolecules.

3. Yeager M, Unger VM, Mitra AK: **Three-dimensional structure of membrane proteins determined by two-dimensional crystallization, electron cryomicroscopy, and image analysis.** *Methods Enzymol* 1999, **294**:135-180.
• This paper describes the practical procedures in studying membrane proteins using electron crystallography.

4. Glaeser RM: **Review: electron crystallography: present excitement, a nod to the past, anticipating the future.** *J Struct Biol* 1999, **128**:3-14.
•• Physical limiting factors, such as radiation damage, the number of images, molecular size and availability of crystals, and their effects on high-resolution structural studies are discussed in detail.

5. Nogales E, Wolf SG, Downing KH: **Structure of the αβ tubulin dimer by electron crystallography.** *Nature* 1998, **391**:199-203.

6. Mitsuoka K, Murata K, Walz T, Hirai T, Agre P, Heymann JB, Engel A, Fujiyoshi Y: **The structure of aquaporin-1 at 4.5 Å resolution reveals short alpha-helices in the center of the monomer.** *J Struct Biol* 1999, **128**:34-43.
• The structure of aquaporin-1 was solved to 4.5 Å resolution by cryo-electron crystallography of 2D crystals. It was found that each subunit consists of a right-handed bundle of six highly tilted transmembrane helices. Sidechains from α helices started to emerge at this resolution.

7. Miyazawa A, Fujiyoshi Y, Stowell M, Unwin N: **Nicotinic acetylcholine receptor at 4.6 Å resolution: transverse tunnels in the channel wall.** *J Mol Biol* 1999, **288**:765-786.
• The nicotinic acetylcholine receptor is a neurotransmitter-gated ion channel that forms well-ordered tubular crystals. From images recorded at 4K with a 300 kV field emission source, the structure of the receptor was established to near-atomic resolution.

8. Zhang P, Toyoshima C, Yonekura K, Green NM, Stokes DL: **Structure of the calcium pump from sarcoplasmic reticulum at 8 Å resolution.** *Nature* 1998, **392**:835-839.

9. Böttcher B, Wynne SA, Crowther RA: **Determination of the fold of the core protein of hepatitis B virus by electron microscopy.** *Nature* 1997, **386**:88-91.

10. Grimes J, Fuller S, Stuart D: **Complementing crystallography: the role of cryo-electron microscopy in structural biology.** *Acta Crystallogr D* 1999, **55**:1742-1749.
• This article discusses the cryo-electron microscopy reconstruction procedure from a crystallographic point of view.

11. He Y, Bowman V, Mueller S, Bator C, Bella J, Peng X, Baker T, Wimmer E, Kuhn R, Rossmann M: **Interaction of the poliovirus receptor with poliovirus.** *Proc Natl Acad Sci USA* 2000, **97**:79-84.

12. Belnap D, McDermott BJ, Filman D, Cheng N, Trus B, Zuccola H, Racaniello V, Hogle J, Steven A: **Three-dimensional structure of poliovirus receptor bound to poliovirus.** *Proc Natl Acad Sci USA* 2000, **97**:73-78.

13. Mueller F, Sommer I, Baranov P, Matadeen R, Stoldt M, Wohnert J, Gorlach M, van Heel M, Brimacombe R: **The 3D arrangement of the 23 S and 5 S rRNA in the *Escherichia coli* 50 S ribosomal subunit based on a cryo-electron microscopic reconstruction at 7.5 Å resolution.** *J Mol Biol* 2000, **298**:35-59.
• The *E. coli* 23S and 5S rRNA of the 50S ribosomal subunit were fitted into an electron density map using the predicted structure of the two rRNAs, as well as cross-linking and footprint data. Crystallographic or NMR structures of seven ribosomal proteins and RNA–protein complexes were also incorporated into the electron microscopy density.

14. Grimes JM, Burroughs JN, Gouet P, Diprose JM, Malby R, Ziéntara S, Mertens PPC, Stuart DI: **The atomic structure of the bluetongue virus core.** *Nature* 1998, **395**:470-478.

15. Prasad B, Hardy M, Dokland T, Bella J, Rossmann M, Estes M: **X-ray crystallographic structure of the Norwalk virus capsid.** *Science* 1999, **286**:287-290.

16. • Reinisch K, Nibert M, Harrison S: **Structure of the reovirus core at 3.6 Å resolution.** *Nature* 2000, **404**:960-967.
The structure of the reovirus core was solved using a 27 Å reconstruction as the initial phasing model. Noncrystallographic fivefold averaging and solvent flattening were used in phase extension.

17. Wang J, Hartling JA, Flanagan JM: **Crystal structure determination of *Escherichia coli* ClpP starting from an EM-derived mask.** *J Struct Biol* 1998, **124**:151-163.

18. Ban N, Freeborn B, Nissen P, Penczek P, Grassucci RA, Sweet R, Frank J, Moore PB, Steitz TA: **A 9 Å resolution X-ray crystallographic map of the large ribosomal subunit.** *Cell* 1998, **93**:1105-1115.

19. DeRosier D, Stokes DL, Darst SA: **Averaging data derived from images of helical structures with different symmetries.** *J Mol Biol* 1999, **289**:159-165.

20. •• Baker TS, Olson NH, Fuller SD: **Adding the third dimension to virus life cycles: three-dimensional reconstruction of icosahedral viruses from cryo-electron micrographs.** *Microbiol Mol Biol Rev* 1999, **63**:862-922.
This paper describes preparation, microscopy and reconstruction methods for icosahedral viral specimens. The paper also discusses the virus life cycle, as illustrated by results from cryo-electron microscopy.

21. • Stewart P, Cary R, Peterson S, Chiu C: **Digitally collected cryo-electron micrographs for single particle reconstruction.** *Microsc Res Tech* 2000, **49**:224-232.
The use of a slow-scan CCD camera for single-particle reconstruction was explored. Experiments on the icosahedral adenovirus (~150 MDa) and the asymmetric DNA-PKcs protein (470 kDa) showed that resolution up to 17 Å was attainable from digitally collected micrographs.

22. Radermacher M: **Weighted back-projection methods.** In *Electron Tomography*. Edited by Frank J. Dordrecht: Plenum Press; 1992:91-115.

23. Chiu CY, Mathias P, Nemerow GR, Stewart PL: **Structure of adenovirus complexed with its internalization receptor, $\alpha_v\beta5$ integrin.** *J Virol* 1999, **73**:6759-6768.

24. McKenna R, Olson NH, Chipman PR, Baker TS, Booth TF, Christensen J, Aasted B, Fox JM, Bloom ME, Wolfinbarger JB *et al.*: **Three-dimensional structure of aleutian mink disease parvovirus: implications for disease pathogenicity.** *J Virol* 1999, **73**:6882-6891.

25. • Yan X, Olson NH, Van Etten JL, Bergoin M, Rossmann MG, Baker TS: **Structure and assembly of large lipid-containing dsDNA viruses.** *Nat Struct Biol* 2000, **7**:101-103.
Two large, lipid-containing icosahedral viruses, each approximately 200 nm in diameter, were studied by cryo-electron microscopy. Reconstruction of these two viruses to 26 Å resolution showed that they each have a triangulation number of 147 and 169.

26. Kolatkar PR, Bella J, Olson NH, Bator CM, Baker TS, Rossmann MG: **Structural studies of two rhinovirus serotypes complexed with fragments of their cellular receptor.** *EMBO J* 1999, **18**:6249-6259.

27. Ferlenghi I, Gowen B, de Haas F, Mancini EJ, Garoff H, Sjöberg M, Fuller SD: **The first step: activation of the Semliki Forest virus spike protein precursor causes a localized conformational change in the trimeric spike.** *J Mol Biol* 1998, **283**:71-81.

28. Tao Y, Olson NH, Xu W, Anderson DL, Rossmann MG, Baker TS: **Assembly of a tailed bacterial virus and its genome release studied in three dimensions.** *Cell* 1998, **95**:431-437.

29. Ibarra B, Caston JR, Llorca O, Valle M, Valpuesta JM, Carrascosa JL: **Topology of the components of the DNA packaging machinery in the phage phi29 prohead.** *J Mol Biol* 2000, **298**:807-815.

30. • Zhang W, Olson N, McKenna R, Baker T: **The structure of maize streak virus: are two heads better than one?** In *Proceeding of Microscopy Microanalysis*; *Portland, Oregon*. Edited by Bailey G. New York: Springer-Verlag, Inc; 1999:1132-1133.
This paper describes the first electron microscopy reconstruction of a Geminivirus particle. The capsid of a Geminivirus consists of two incomplete icosahedra.

31. • Rossmann MG, Tao Y: **Cryo-electron-microscopy reconstruction of partially symmetric objects.** *J Struct Biol* 1999, **125**:196-208.
This paper describes a reconstruction procedure for particles with low symmetry. The best orientation of an object is determined on the basis of self-rotation function.

32. Crowther RA, DeRosier DJ, Klug A: **The reconstruction of a three-dimensional structure from projections and its application to electron microscopy.** *Proc R Soc Lond B Biol Sci* 1970, **317**:319-340.

33. Gomez-Lorenzo M, Spahn C, Agrawal R, Grassucci R, Penczek P, Chakraburtty K, Ballesta J, Lavandera J, Garcia-Bustos J, Frank J: **Three-dimensional cryo-electron microscopy localization of EF2 in the *Saccharomyces cerevisiae* 80S ribosome at 17.5 Å resolution.** *EMBO J* 2000, **19**:2710-2718.

34. Beuron F, Maurizi MR, Belnap DM, Kocsis E, Booy FP, Kessel M, Steven AC: **At sixes and sevens: characterization and the symmetry mismatch of the ClpAP chaperone-assisted protease.** *J Struct Biol* 1998, **123**:248-259.

35. • Llorca O, McCormack E, Hynes G, Grantham J, Cordell J, Carrascosa J, Willison K, Fernandez J, Valpuesta J: **Eukaryotic type II chaperonin CCT interacts with actin through specific subunits.** *Nature* 1999, **402**:693-696.
The interaction between the chaperonin CCT and its substrate was studied by 3D cryo-electron microscopy.

36. Andel F III, Ladurner A, Inouye C, Tjian R, Nogales E: **Three-dimensional structure of the human TFIID-IIA-IIB complex.** *Science* 1999, **286**:2153-2156.

37. Nield J, Orlova E, Morris E, Gowen B, van Heel M, Barber J: **3D map of the plant photosystem II supercomplex obtained by cryoelectron microscopy and single particle analysis.** *Nat Struct Biol* 2000, **7**:44-47.

38. Sharma M, Jeyakumar L, Fleischer S, Wagenknecht T: **Three-dimensional structure of ryanodine receptor isoform three in two conformational states as visualized by cryo-electron microscopy.** *J Biol Chem* 2000, **275**:9485-9491.

39. Orlova E, Dube P, Beckmann E, Zemlin F, Lurz R, Trautner T, Tavares P, van Heel M: **Structure of the 13-fold symmetric portal protein of bacteriophage SPP1.** *Nat Struct Biol* 1999, **6**:842-846.

40. Orlova E, Rahman M, Gowen B, Volynski K, Ashton A, Manser C, van Heel M, Ushkaryov Y: **Structure of alpha-latrotoxin oligomers reveals that divalent cation-dependent tetramers form membrane pores.** *Nat Struct Biol* 2000, **7**:48-53.

41. Kong LB, Siva AC, Rome LH, Stewart PL: **Structure of the vault, a ubiquitous cellular component.** *Structure* 1999, **7**:371-379.

42. van Heel M: **Unveiling ribosomal structures: the final phases.** *Curr Opin Struct Biol* 2000, **10**:259-264.

43. Henderson R: **The potential and limitations of neutrons, electrons, and X-rays for atomic resolution microscopy of unstained biological molecules.** *Q Rev Biophys* 1995, **28**:171-193.

44. • de Haas F, Paatero A, Mindich L, Bamford D, Fuller S: **A symmetry mismatch at the site of RNA packaging in the polymerase complex of dsRNA bacteriophage ϕ6.** *J Mol Biol* 1999, **294**:357-372.
In the phage ϕ6 nucleocapsid, a sixfold symmetric substructure (~300 kDa) attaches to each of the fivefold axes. The symmetry mismatch between the substructure and the rest of the nucleocapsid was investigated by electron microscopy reconstruction with or without symmetry-imposed averaging.

45. Stoddard B: **New results using Laue diffraction and time-resolved crystallography.** *Curr Opin Struct Biol* 1998, **8**:612-618.

46. Moffat K, Henderson R: **Freeze trapping of reaction intermediates.** *Curr Opin Struct Biol* 1995, **5**:656-663.

47. White HD, Walker ML, Trinick J: **A computer-controlled spraying-freezing apparatus for millisecond time-resolution electron cryomicroscopy.** *J Struct Biol* 1998, **121**:306-313.

48. Trachtenberg S: **A fast-freezing device with a retractable environmental chamber, suitable for kinetic cryo-electron microscopy studies.** *J Struct Biol* 1998, **123**:45-55.

49. • Lata R, Conway J, Cheng N, Duda R, Hendrix R, Wikoff W, Johnson J, Tsuruta H, Steven A: **Maturation dynamics of a viral capsid: visualization of transitional intermediate states.** *Cell* 2000, **100**:253-263.
The dynamic process of viral capsid maturation was studied by cryo-electron microscopy. Reconstructions were obtained from samples that had proceeded to different stages of maturation.

50. Stark H, Rodnina M, Wieden H, van Heel M, Wintermeyer W: **Large-scale movement of elongation factor G and extensive conformational change of the ribosome during translocation.** *Cell* 2000, **100**:301-309.

Thiostrepton-stalled elongation factor G–ribosome–tRNA complexes, frozen in both pre-translocation and post-translocation states, were studied by cryo-electron microscopy. 3D reconstructions revealed that elongation factor G experiences extensive reorientation and the structure of the ribosome 30S subunit changed substantially.

51. Baumeister W, Grimm R, Walz J: **Electron tomography of molecules and cells.** *Trends Cell Biol* 1999, **9**:81-85.

52. Nicastro D, Frangakis AS, Typke D, Baumeister W: **Cryo-electron tomography of Neurospora mitochondria.** *J Struct Biol* 2000, **129**:48-56.

A whole, frozen-hydrated mitochondria was studied by cryo-electron tomography to approximately 6.8 nm resolution. In a 3D reconstruction of an 'inside-out vesicle', F_0F_1 particles were identified. This work demonstrates the possibility of 'molecular resolution' in tomography in the near feature.

53. Ladinsky M, Mastronarde D, McIntosh J, Howell K, Staehelin L: **Golgi structure in three dimensions: functional insights from the normal rat kidney cell.** *J Cell Biol* 1999, **144**:1135-1149.

54. Conway JF, Cheng N, Zlotnick A, Wingfield PT, Stahl SJ, Steven AC: **Visualization of a 4-helix bundle in the hepatitis B virus capsid by cryo-electron microscopy.** *Nature* 1997, **386**:91-94.

55. Trus BL, Roden RBS, Greenstone HL, Vrhel M, Schiller JT, Booy FP: **Novel structural features of bovine papillomavirus capsid revealed by a three-dimensional reconstruction to 9 Å resolution.** *Nat Struct Biol* 1997, **4**:413-420.

56. Mancini EJ, Clarke M, Gowen BE, Rutten T, Fuller SD: **Cryo-electron microscopy reveals the functional organization of an enveloped virus, Semliki Forest virus.** *Mol Cell* 2000, **5**:255-266.

57. Matadeen R, Patwardhan A, Gowen B, Orlova E, Pape T, Cuff M, Mueller F, Brimacombe R, van Heel M: **The *Escherichia coli* large ribosomal subunit at 7.5 Å resolution.** *Structure* 1999, **7**:1575-1583.

A completely asymmetric structure was determined to beyond 10 Å by single-particle cryo-electron microscopy reconstruction.

58. Zhou ZH, Dougherty M, Jakana J, He J, Rixon FJ, Chiu W: **Seeing the herpesvirus capsid at 8.5 Å.** *Science* 2000, **288**:877-880.

The structure of the herpesvirus capsid, approximately 125 nm in diameter, was solved to 8.5 Å resolution.

59. Gabashvili I, Agrawal R, Spahn C, Grassucci R, Svergun D, Frank J, Penczek P: **Solution structure of the *E. coli* 70S ribosome at 11.5 Å resolution.** *Cell* 2000, **100**:537-549.

60. Conway JF, Steven AC: **Methods for reconstructing density maps of 'single' particles from cryoelectron micrographs to subnanometer resolution.** *J Struct Biol* 1999, **128**:106-118.

The authors considered contrast transfer function correction and combining data from micrographs at different underfocus levels as the major reasons for achieving subnanometer resolution in their work on the hepatitis B viral capsid. Implementation of these procedures is discussed.

61. Penczek P, Ban N, Grassucci RA, Agrawal RK, Frank J: ***Haloarcular marismortui* 50S subunit-complementarity of electron microscopy and X-ray crystallographic information.** *J Struct Biol* 1999, **128**:44-50.

A comparison of rotationally averaged power spectra of the 50S subunit ribosome structure obtained from X-ray crystallography and electron microscopy reconstruction showed that, in electron microscopy, Fourier amplitudes were progressively underestimated at higher spatial frequencies. Fourier amplitudes of the cryo-map were corrected on the basis of the rotational spectra from X-ray crystallography, resulting in enhancement of structural details.

62. Schmid M, Sherman M, Matsudaira P, Tsuruta H, Chiu W: **Scaling structure factor amplitudes in electron cryomicroscopy using X-ray solution scattering.** *J Struct Biol* 1999, **128**:51-57.

The authors used intensity profiles from X-ray solution scattering to scale Fourier amplitudes of a 3D reconstruction and obtained an electron density map that was more physically interpretable.

63. Brink J, Gross H, Tittmann P, Sherman M, Chiu W: **Reduction of charging in protein electron cryomicroscopy.** *J Microsc* 1998, **191**:67-73.

64. Safer D: **Undecagold cluster labeling of proteins at reactive cysteine residues.** *J Struct Biol* 1999, **127**:101-105.

65. Hainfeld JF, Liu W, Halsey CMR, Freimuth P, Powell RD: **Ni-NTA-Gold clusters target his-tagged proteins.** *J Struct Biol* 1999, **127**:185-198.

66. Spahn C, Grassucci R, Penczek P, Frank J: **Direct three-dimensional localization and positive identification of RNA helices within the ribosome by means of genetic tagging and cryo-electron microscopy.** *Structure* 1999, **7**:1567-1573.

67. Conway JF, Cheng N, Zlotnick A, Stahl SJ, Wingfield PT, Steven AC: **Localization of the N terminus of hepatitis B virus capsid protein by peptide-based difference mapping from cryoelectron microscopy.** *Proc Natl Acad Sci USA* 1998, **95**:14622-14627.

68. Che Z, Olson NH, Leippe D, Lee W-M, Mosser AG, Rueckert RR, Baker TS, Smith TJ: **Antibody-mediated neutralization of human rhinovirus 14 explored by means of cryoelectron microscopy and X-ray crystallography of virus-Fab complexes.** *J Virol* 1998, **72**:4610-4622.

69. Bella J, Kolatkar P, Marlor C, Greve J, Rossmann M: **The structure of the two amino-terminal domains of human intercellular adhesion molecule-1 suggests how it functions as a rhinovirus receptor.** *Virus Res* 1999, **62**:107-117.

70. Rossmann MG: **The molecular replacement method.** *Acta Crystallogr A* 1990, **46**:73-82.

71. Kisseberth N, Brauer G, Grosser B, Potter CS, Carragher B: **JavaScope: a web-based TEM control interface.** *J Struct Biol* 1999, **125**:229-234.

72. Hadida-Hassan M, Young SJ, Peltier ST, Wong M, Lamont S, Ellisman MH: **Web-based telemicroscopy.** *J Struct Biol* 1999, **125**:235-245.

73. Ermantraut E, Wohlfart K, Tichelaar W: **Perforated support foils with pre-defined hole size, shape and arrangement.** *Ultramicroscopy* 1998, **74**:75-81.

74. Pulokas J, Green C, Kisseberth N, Potter CS, Carragher B: **Improving the positional accuracy of the goniometer on the Philips CM series TEM.** *J Struct Biol* 1999, **128**:250-256.

75. Boier Martin I, Marinescu D, Lynch R, Baker T: **Identification of spherical virus particles in digitized images of entire electron micrographs.** *J Struct Biol* 1997, **120**:146-147.

76. Thuman-Commike PA, Chiu W: **PTOOL: a software package for the selection of particles from electron cryomicroscopy spot-scan images.** *J Struct Biol* 1996, **116**:41-47.

77. Zhou ZH, Chiu W, Haskell K, Spears HJ, Jakana J, Rixon FJ, Scott LR: **Refinement of herpesvirus B-capsid structure on parallel supercomputers.** *Biophys J* 1998, **74**:576-588.

78. Volkmann N, Hanein D: **Quantitative fitting of atomic models into observed densities derived by electron microscopy.** *J Struct Biol* 1999, **125**:176-184.

79. Wriggers W, Milligan RA, McCammon JA: **Situs: a package for docking crystal structures into low-resolution maps from electron microscopy.** *J Struct Biol* 1999, **125**:185-195.

80. Sosinsky GE, Baker TS, Hand G, Ellisman MH: **The electron microscopy outreach program: a web based resource for research and education.** *J Struct Biol* 1999, **125**:246-252.

81. Carazo JM, Stelzer EHK: **The BioImage database project: organizing multidimensional biological images in an object-relational database.** *J Struct Biol* 1999, **125**:97-102.

The BioImage database organizes multidimensional images from various kinds of microscopy techniques, for example, atomic force microscopy images (2D), transmission electron microscopy reconstructions (3D) and animations (4D).

82. Zhu J, Penczek PA, Schröder R, Frank J: **Three-dimensional reconstruction with contrast transfer function correction from energy-filtered cryoelectron micrographs: procedure and application to the 70S *Escherichia coli* ribosome.** *J Struct Biol* 1997, **118**:197-219.

83. Thuman-Commike PA, Chiu W: **Reconstruction principles of icosahedral virus structure determination using electron cryomicroscopy.** *Micron* 2000, **31**:687-711.

This paper provides detailed descriptions of various data-processing steps leading to three-dimensional reconstruction of icosahedral viruses.